Pramāṇa – J. Phys., Vol. 35, No. 1, July 1990, pp. 105–114. © Printed in India.

Experimental investigation of angular dependence of photon induced L-shell X-ray emission intensity

K S KAHLON, K SHATENDRA*, K L ALLAWADHI and B S SOOD

Nuclear Science Laboratories, Department of Physics, Punjabi University, Patiala 147002, India

*Solid State Physics Laboratory, Lucknow Road, Delhi 110007, India

MS received 27 November 1989

Abstract. The angular dependence of emission intensity of L shell X-rays induced by 59·57 keV photons in Pb and U is investigated by measuring the normalized intensities of the resolved L X-ray peaks at different angles varying from 40° to 120°. It is observed that while L_l and L_α X-ray peaks (originating from $J = 3/2$ state) show some anisotropic angular distribution, the emission of L_β and L_γ X-ray peaks is isotropic. The present results contradict the calculations of Co-oper and Zare (1969) that after photoionization of inner shell, the vacancy state has equal population of magnetic substates and the subsequent X-ray emission is isotropic but confirm the predictions of Flugge *et al* (1972) that the atomic inner shell vacancies produced after photoionization are aligned and the x-ray emission from the filling of vacancies in state with $J \geqslant 3/2$ is anisotropic.

Keywords. Photoionization; inner-shell vacancies; Fluorescent L shell X-rays; angular distribution.

PACS No. 32·80

1. Introduction

Contrary to the predictions of Co-oper and Zare (1969) that after photoionization of inner shell, the vacancy state has equal population of different magnetic substates and the subsequent emission of X-rays is isotropic, the theoretical calculations by Flugge *et al* (1972) have shown that after the ionization of inner shells by an unpolarized photon beam, the state of ion thus formed turns out to be aligned i.e. it has unequal population of different magnetic substates if its total angular momentum $J > 1/2$. This alignment is manifested by the anisotropic emission of characteristic X-rays or Auger electrons from such state. Therefore, the X-rays originating from the states corresponding to $J = 1/2$ (K-shell and L_I, L_{II}, M_I, M_{II} subshells etc.) are expected to be isotropic and those corresponding to state $J = 3/2$ (e.g. L_{III}, M_{III} and M_{IV} subshells) and $J = 5/2$ (e.g. M_V subshell) are expected to be anisotropic in their spatial distribution.

The angular distribution of ion induced K and L shell X-rays has been extensively investigated by many workers and some measurable anisotropy in L_l and L_α X-rays induced by ions of different energies has been observed in some elements (Middlemann *et al* 1970; Hardy *et al* 1970; Codling *et al* 1976; Stoller *et al* 1977; Palinkas *et al* 1979; Jitschin *et al* 1979a, b; Ellsworth *et al* 1979; Kabachnik *et al* 1980; Baros Leute *et al* 1982; Forrest *et al* 1983; Papp and Palinkas 1988). However, to the best of our

knowledge, no measurement of angular distribution of photon induced X-rays in any element has been reported to date. To check the predictions of Flugge *et al* (1972) we have measured the intensities of L_l, L_α, L_β and L_γ groups of L X-ray lines at different emission angles θ in the angular range of 40° to 120° relative to the intensity at 90° in Pb and U induced by 59·57 keV photons. The experimental set up, method of measurement and results are reported in this paper.

2. Method of measurement

The L-shell X-ray lines are not completely resolved corresponding to their individual subshell transitions by the present available energy dispersive spectrometers due to their limited resolution. However, the L X-ray lines of a heavy element appear under four distinct peaks corresponding to L_l, L_α, L_β and L_γ groups of lines well resolved from each other. Out of these four peaks, only L_l and L_α originate purely from the transitions to L_{III} subshell ($J = 3/2$) and are thus expected to show anisotropic emission, if any. The L_β peak of X-rays also contains some contributions from L_{III} subshell but most of its intense constituent lines originate from L_I and L_{II} subshells ($J = 1/2$), therefore, this peak cannot provide a significant clue to the anisotropic emission of L_{III} subshell X-rays. However, L_γ X-ray peak contains only the contributions from L_I and L_{II} subshells ($J = 1/2$) and is therefore expected to be isotropically emitted. The anisotropy of L shell X-rays can be investigated by measuring the absolute differential cross-sections for the emission of L X-rays at various angles with respect to the incident photom beam. However, this method will involve the uncertainties in the measurements of the absolute values of source strength, solid angles, efficiency of detector, target thickness, absorption coefficients etc. The accuracy of measurements is considerably improved by measuring the relative intensities of resolved L X-ray peaks instead of their absolute values, because only the ratios of counting rates, target self-absorption correction factors and the solid angles have to be determined.

The number of X-rays detected under the ith L X-ray peak along a direction making an angle θ (X-ray emission angle) with the photon beam is given as

$$N_x^\theta(L_i) = S(\gamma)\frac{\omega_1}{4\pi}a(\gamma)\frac{N}{M}t\beta^\theta(L_i)\left(\frac{d\sigma^\theta}{d\Omega}\right)_{expt}\omega_2^\theta\epsilon(L_i) \tag{1}$$

where $(d\sigma^\theta/d\Omega)L_i$ is differential cross-section for the emission of X-rays under the L_i peak $S(\gamma)$ is the intensity of gamma rays emitted from the source $a(\gamma)$ is the correction for absorption of gamma rays in source, air column, etc N is the Avogadro's number M is the atomic weight of the target element t is the thickness of the target in g/cm^2 $\beta_L(\gamma)$ is the correction factor to take into account the absorption of incident radiations and emitted X-rays in the target. ω_1 and ω_2 are the target-source and target-detector solid angles and $\varepsilon(L_i)$ is the photo-peak efficiency of the detector. ω_1 is independent of θ because the angle of incidence is kept fixed throughout the experiment. The ratio of intensity $I^\theta(L_i)$ measured at an emission angle θ to the intensity $I^{90}(L_i)$ measured at an emission angle 90°, is therefore, given

$$\frac{d\sigma^\theta(L_i)}{d\sigma^{90}(L_i)} = \frac{I^\theta(L_i)}{I^{90}(L_i)} = \frac{N_x^\theta(L_i)}{N_x^{90}(L_i)}\frac{\beta^{90}(L_i)}{\beta^\theta(L_i)}\frac{\omega_2^{90}}{\omega_2^\theta}. \tag{2}$$

Thus the intensity ratio $I^{\theta}(L_i)/I^{90}(L_i)$ can be measured at various emission angles θ by determining the ratios of counts per unit time under L_i X-ray peak, self-absorption correction factors of target and solid angles.

3. Experimental set-up and measurement

The experimental arrangement used to investigate the angular distribution of photon induced fluorescent X-rays is shown in figure 1. A fine collimated beam of 59·57 keV photons from ~100 mCi ^{241}Am radioactive source was allowed to fall on the targets of elements under investigation. The angle of incidence was kept fixed at 70° while the angle at which fluorescent X-rays were detected with respect to the incident beam was varied by moving the source-target assembly together along a turn table as shown in figure 1. The detector being heavy and fragile was not moved. The L and higher shell vacancies were produced in target elements by photoionization. The K-shells of the target elements were not excited since the K edge energies were higher than 59·57 keV. The fluorescent L shell X-rays emitted from the targets were analyzed by an EG and G ORTEC Si(Li) detector coupled to an ND 76 multichannel analyzer coupled to it. The overall resolution of the spectrometer was ~300 eV at 5·9 keV. The source and target assemblies were together mounted on a movable turn table with a graduated angular scale to read the angular rotation. The experimental arrangement was designed to obtain the variation of emission angle θ from 40° to 120° with angular spread of ±2·5°. These limits on the angles were imposed by the size of collimator and relative distances between source, target and detector. The measurements were carried out at nine angles at angular intervals of 10°. To measure the ratio of counting rates $N_x^{\theta}(L)/N_x^{90°}(L)$ 99·9% pure metallic targets of Pb and U

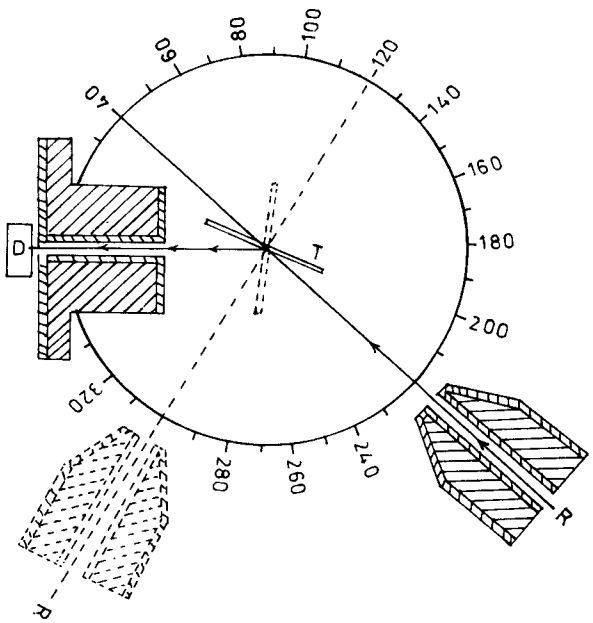

Figure 1. Experimental set up used for the investigation of angular distribution of L shell fluorescent X-rays. R-radioactive source (^{241}Am), T-target, D-detector Si(Li).

were irradiated with 59·57 keV photons in the experimental set-up and the emitted fluorescent L shell X-rays were detected at different emission angles by rotating the source target assembly. The background due to natural radioactivity from U target was taken into account as discussed earlier (Kumar *et al* 1985). The experiment with each target at one emission angle was run for a long time to obtain statistical accuracy $\sim 1\%$ for L_α and L_β peaks, 2 to 3% for L_l and L_γ peaks. Typical spectra of L shell X-rays of Pb at emission angle $\theta = 90°$ is shown in figure 2. The values of ratios of target self-absorption correction factor $\beta^{90}(L_i)/\beta^{\theta}(L_i)$ were calculated as discussed in Kumar *et al* (1982).

The ratios at different angles were also determined experimentally for lead. Six targets of lead of thickness varying from 14·5 to 33 mg/cm^2 were used and counts under the L_α and L_β peaks were recorded at each angle. The variation of number of counts under the L_α peak of Pb against target thickness at emission angles of 70° and 120° are shown in figure 3a, b. The values of counts $N(t_1)$ and $N(t_2)$ corresponding to thickness t and $2t$ below saturation thickness were read from the plot of counts against thickness (figure 3) and the value of β^{θ} determined from the relation

$$\beta^{\theta} = \frac{2 - 2\dfrac{N^{\theta}(t_2)}{N^{\theta}(t_1)}}{\ln\left[N^{\theta}(t_1)/(N^{\theta}(t_2) - N^{\theta}(t_1))\right]}.$$

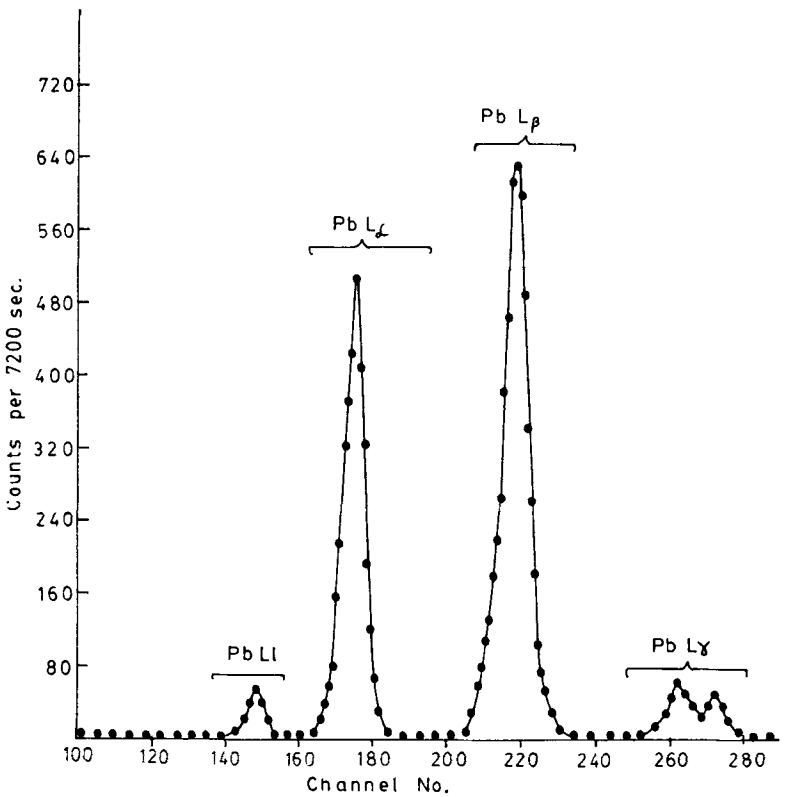

Figure 2. Spectrum of Pb L X-rays recorded with Si(Li) X-ray spectrometer at emission angle of 90°.

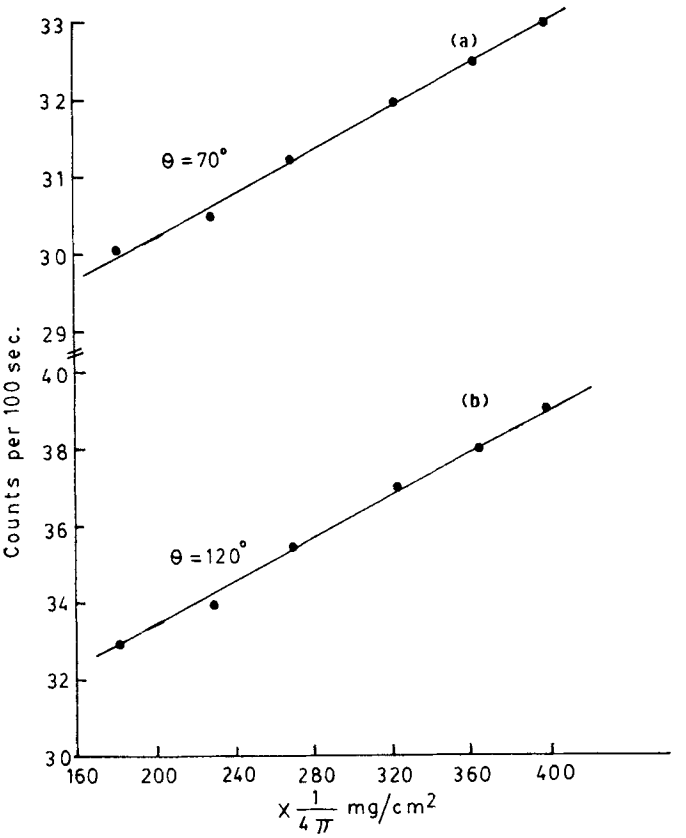

Figure 3. Variation of number of counts under L_β X-ray peak of lead targets against the thickness of targets at emission angles of 70° and 120°.

Table 1. Comparison of experimental and calculated values of self absorption correction factor.

θ in degrees	$\beta^\theta(L_\alpha)/\beta^{90}(L_\alpha)$		$\beta^\theta(L_\beta)/\beta^{90}(L_\beta)$	
	Experimental	Calculated	Experimental	Calculated
50	0·63 ± 0·0071	0·63	0·58 ± 0·005	0·58
70	0·85 ± 0·01	0·86	0·85 ± 0·009	0·84
90	1·00 ± 0·01	1·00	1·00 ± 0·009	1·00
120	1·04 ± 0·01	1·03	1·03 ± 0·01	1·04

The experimental values of $\beta^\theta(L_\alpha)/\beta^{90}(L_\alpha)$ and $\beta^\theta(L_\beta)/\beta^{90}(L_\beta)$ are compared with their theoretically calculated values in table 1 and found to agree with each other within experimental errors. The ratios of target to detector solid angles were measured in a separate experiment which is described below.

The experimental targets of Pb and U are replaced by a suitable low Z element (Mo; Z = 42) whose K shell threshold energy lies below 59·57 keV. The K shell X-rays of Mo are produced by photoionization of K shell. The K shell X-rays are detected in the same experimental set-up at various emission angles. Assuming isotropic

emission of K X-rays the number of X-rays detected under K peak at emission angle of θ are given as

$$N_x^{\theta}(K_\alpha) = S\frac{\omega_1}{4\pi}a(\gamma)\frac{N}{M}t\beta^{\theta}(K_\alpha)\sigma_k^x\frac{\omega_2^{\theta}}{4\pi}\varepsilon(K_\alpha) \tag{3}$$

where σ_K^x is the integral K X-ray emission cross-section. All other terms have their usual meaning for K shell X-rays. Since the K shell X-rays originate from a state with $J = 1/2$, these radiations should have an isotropic angular distribution (McFarlane 1972; Berzhko and Kabachnik 1977) which has also been experimentally verified by us. Therefore, it can be safely concluded that $I^{\theta}(K_\alpha) = I^{90}(K_\alpha)$ and $\omega_2^{90}/\omega_2^{\theta}$ may be written as

$$\frac{\omega_2^{90}}{\omega_2^{\theta}} = \frac{N_x^{90}(K_\alpha)}{N_x^{\theta}(K_\alpha)}\frac{\beta^{\theta}(K_\alpha)}{\beta^{90}(K_\alpha)}. \tag{4}$$

Thus the ratio $\omega_2^{90}/\omega_2^{\theta}$ was determined by using calculated values of $\beta(K_\alpha)$ and measured values of counting rates under K peak at different emission angles. The spectrum for Mo K shell X-rays at each angle of emission was recorded for a long time so as to get the statistical accuracy of less than 1%. The typical K shell X-ray spectra of Mo at emission angle $\theta = 90°$ is shown in figure 4. The values of $\omega_2^{90}/\omega_2^{\theta}$ as determined from (4) are listed in table 2.

4. Results and discussion

The measured values of intensity ratios $I^{\theta}(L_i)/I^{90}(L_i)$ at emission angle θ varying from 40° to 120° in elements Pb and U are given in table 3. The uncertainties in the present measurements are 8–10% which are mainly due to the uncertainties in counting rates, target self-absorption correction factor and the measurement of ratio of solid angles. It is seen that the L_γ X-ray peak is isotropically emitted as expected by the theory since it consists of the transitions from $L_I(J = 1/2)$ and $L_{II}(J = 1/2)$ subshells. However, though the L_β peak contains some contributions from L_{III} $(J = 3/2)$ subshell transitions, yet it does not show any measurable anisotropy. Thus L_β peak can also be said to be isotropically emitted within the uncertainties of present measurements. The L_l and L_α X-ray peaks which contain contributions only from L_{III} subshell $(J = 3/2)$ show measureable anisotropy. The observed anisotropy of L_l peak is more than that of L_α peak because the L_l peak contains one intense line (L_{III}-M_I) but L_α peak contains $L\alpha_1$ (L_{III}-M_{III}) and $L\alpha_2$ (L_{III}-M_{IV}) lines of opposite anisotropy with relative intensity of 100 and 114 respectively (Storm and Israel 1970). Assuming the intensity at any angle θ $I^{\theta}(L_i)$ for any group of X-rays Li to be represented by a Legendre polynomial sum

$$I(\theta) = \sum_l a_l P_l(\cos\theta)$$

the observed intensity ratios $I^{\theta}(L_i)/I^{90}(L_i)$ are fitted to the relation

$$I^{\theta}(L_i)/I^{90}(L_i) = \textstyle\sum_{n=1}^{2} 1 + a_n \cos^n\theta$$

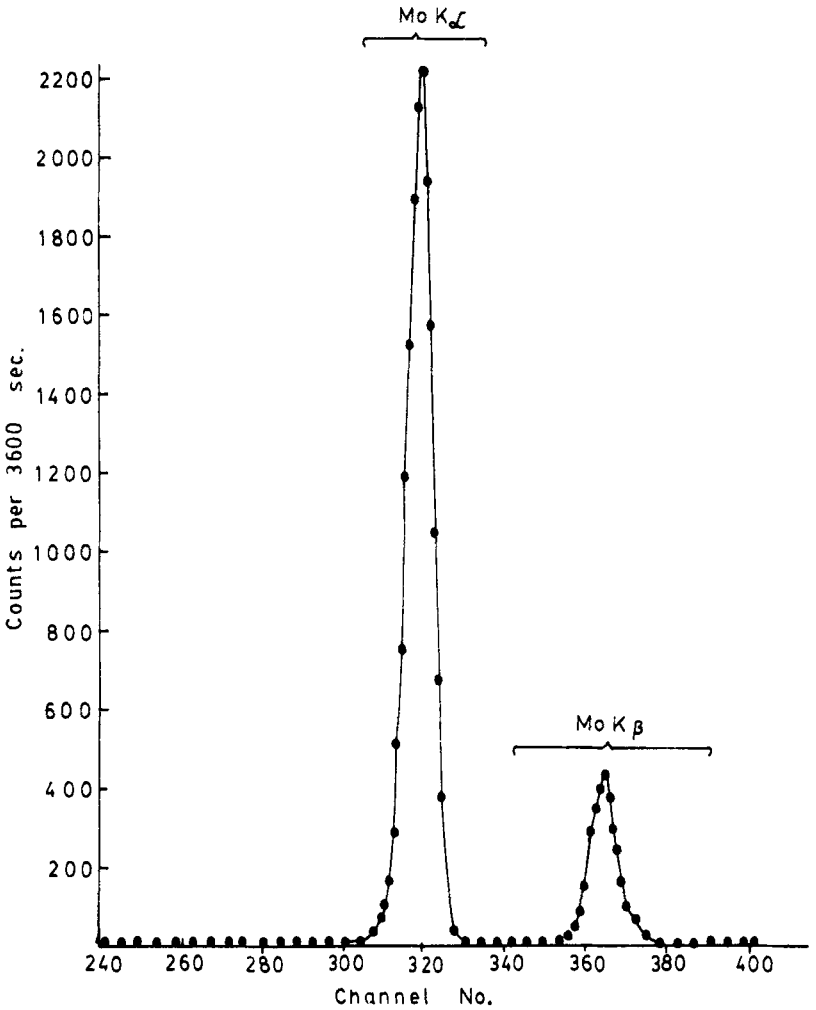

Figure 4. Spectrum of Mo K X-rays recorded with Si(Li) X-ray spectrometer at emission angle of 90 .

Table 2. Experimental values of target-detector solid angles.

Angle of emission	$\omega_2^{90}/\omega_2^{\theta}$
40	0·55±0·03
50	0·63±0·03
60	0·71±0·04
70	0·85±0·04
80	0·92±0·05
90	1·00±0·06
100	1·00±0·06
110	1·00±0·06
120	0·97±0·06

Table 3. Experimental values of normalized L-shell X-ray intensity ratios.
i) For Pb

θ (in deg)	$I^{\theta}(L_l)/I^{90}(L_l)$	$I^{\theta}(L_\alpha)/I^{90}(L_\alpha)$	$I^{\theta}(L_\beta)/I^{90}(L_\beta)$	$I^{\theta}(L_\gamma)/I^{90}(L_\gamma)$
40	1·63±0·15	1·29±0·12	1·00±0·09	0·99±0·09
50	1·46±0·13	1·24±0·12	1·02±0·10	1·00±0·10
60	1·33±0·12	1·20±0·11	1·01±0·10	0·92±0·09
70	1·23±0·11	1·16±0·11	1·00±0·09	1·00±0·10
80	1·22±0·10	1·08±0·10	1·00±0·09	0·95±0·09
90	1·00±0·09	1·00±0·09	0·96±0·09	0·95±0·09
100	0·91±0·09	0·93±0·09	1·01±0·09	1·00±0·10
110	0·86±0·08	0·88±0·09	1·00±0·09	0·95±0·09
120	0·81±0·08	0·85±0·08	1·00±0·09	1·05±0·10

ii) For U

θ (in deg)	$I^{\theta}(L_l)/I^{90}(L_l)$	$I^{\theta}(L_\alpha)/I^{90}(L_\alpha)$	$I^{\theta}(L_\beta)/I^{90}(L_\beta)$	$I^{\theta}(L_\gamma)/I^{90}(L_\gamma)$
40	1·80±0·18	1·16±0·12	0·99±0·10	1·00±0·10
50	1·62±0·16	1·13±0·11	0·99±0·10	0·99±0·10
60	1·42±0·14	1·09±0·11	1·00±0·10	0·99±0·10
70	1·27±0·12	1·07±0·10	1·01±0·10	1·03±0·10
80	1·12±0·11	1·04±0·10	0·99±0·10	1·01±0·10
90	1·00±0·11	1·00±0·10	1·00±0·10	1·00±0·10
100	0·88±0·08	0·96±0·10	0·99±0·10	1·01±0·10
110	0·77±0·08	0·93±0·09	0·99±0·10	0·99±0·10
120	0·62±0·06	0·91±0·09	1·00±0·10	1·00±0·10

The values of the coefficients for Pb and U are listed in table below:

Elements	Pb		U	
Peaks	L_l	L_α	L_l	L_α
a_1	0·56	0·33	0·8	0·2
a_2	0·35	0·06	0·08	0·02

The experimental values and the fitted curve for the intensity ratios are shown in figure (5a–f). The present results contradict the predictions of Co-oper and Zare (1969) but confirm those of Flugge *et al* (1972). From the present measurements it is also seen that the anisotropy depends upon the atomic number of the target element. The anisotropy of L_l and L_α groups of L X-rays lines, according to Flugge *et al* arises from the unequal population of the magnetic substates of L_3 subshell vacancy state created after photo-ionization. The population distribution of the magnet substates of the L_3 subshell vacancy state is governed by their photo-ionization cross-sections which depends upon the atomic number of the target element and the energy of the incident photon. The observed Z dependence of the anisotropy is thus also explained by the calculations of Flugge *et al*. Further experiments are in progress to investigate the details of Z and energy dependence.

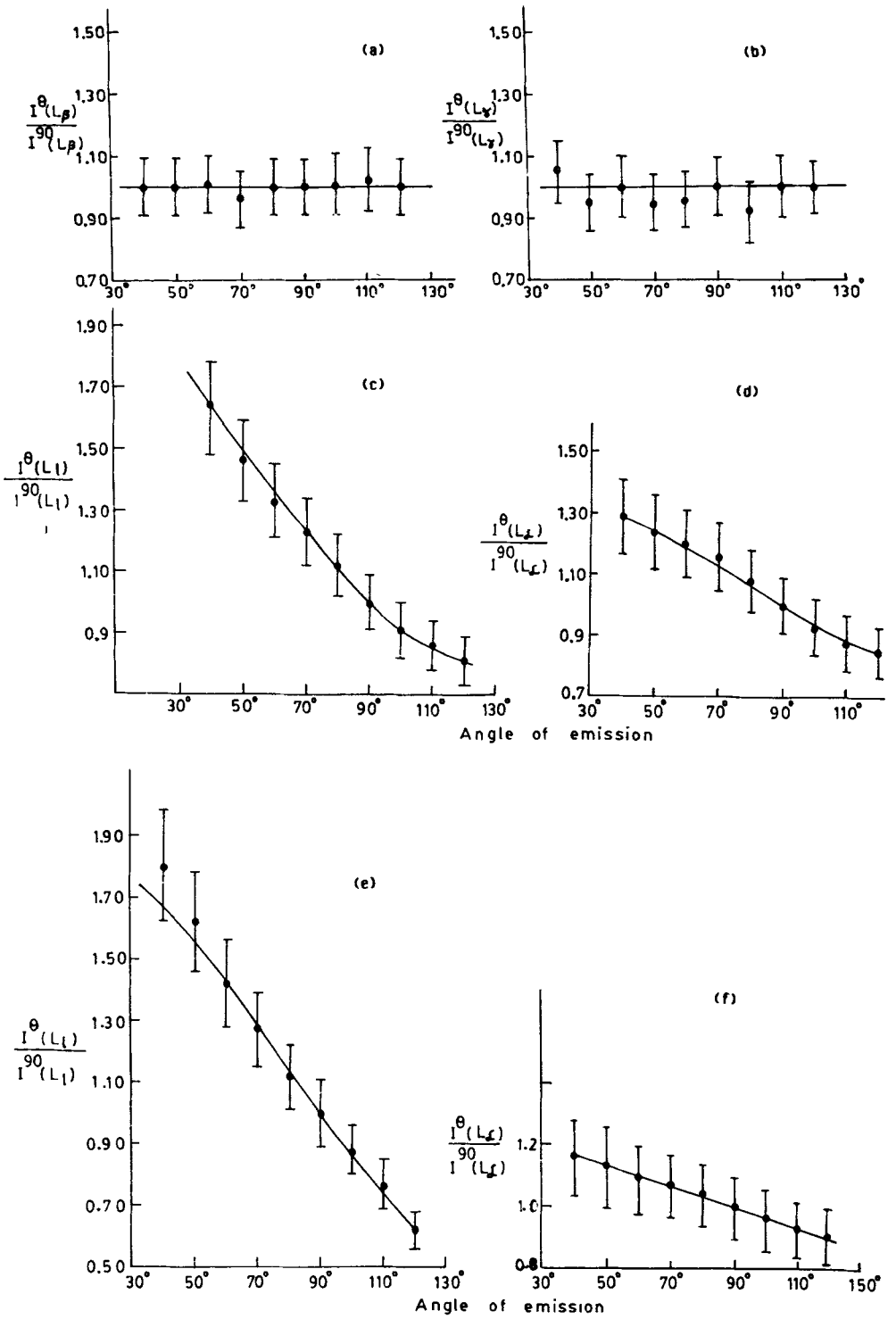

Figure 5. Variation of relative intensities $I^{\theta}(L_i)/I^{90}(L_i)$ of L subshell fluorescent X-rays of Pb and U with emission angle θ. Figures a, b, e, f for U and figures c and d for Pb.

Acknowledgements

Financial support from the Department of Science and Technology and University Grants Commission, India, is gratefully acknowledged.

References

Barros Leute C V, deCartro Faria N V, Horowicz R J, Montenegro E C and de Pinho A G 1982 *Phys. Rev.* **A25** 1880
Berezhko E G and Kabachnik N M 1977 *J. Phys.* **B10** 2467
Codling K, Houlgate R G, Westand J B and Woodruff P R 1976 *J. Phys.* **B9** L83
Co-oper J and Zare R N 1969 *Atomic collision processes* (New York: Gordon and Breach), vol. xic, 317
Ellsworth L D, Doyle B L, Schiebel U and McDonald J R 1979 *Phys. Rev.* **A19** 943
Flugge S, Mehlhorn W and Schmidt V 1972 *Phys. Rev. Lett.* **29** 7
Forrest L F, James G K, Ross K J and Pejeev V 1983 *J. Phys.* **B16** 467
Hardy J, Hennins A and Bearden J A 1970 *Phys. Rev.* **A2** 1708
Jitschin W, Kleinpoppen H, Hippler R and Lutz H O 1979a *J. Phys.* **B12** 4077
Jitschin W, Hippler R, Shanker R, Kleinpoppen H, Schuch R and Lutz H O 1979b *J. Phys.* **B16** 1417
Kabachnik N M, Petukhov Y P, Romanovaski E A and Sizov V V 1980 *Sov. Phys. JETP* **51** 869
Kumar S, Allawadhi K and Sood B S 1985 *Phys. Rev.* **A31** 2918
Kumar Shatindra, Mittal R, Allawadhi K L and Sood B S 1982 *J. Phys.* **B15** 3377
McFarlane S C 1972 *J. Phys.* **B5** 1906
Middlemann L M, Ford R L and Hofsta R 1970 *Phys. Rev.* **A2** 1429
Palinkas J, Schlenk B and Valek A 1979 *J. Phys.* **B12** 3273
Papp T and Palinkas J 1988 *Phys. Rev.* **A38** 2686
Stoller C, Wolfli W, Bonani G, Stockli M and Suter M 1977 *J. Phys.* **B10** L347
Storm E and Israel 1970 *Nucl. Data Tables* **A7** 565